

## APPROACH TO THE FERROMAGNETIC SATURATION OF THE Fe<sub>39</sub>Co<sub>33</sub>Y<sub>8</sub>B<sub>20</sub> ALLOY PRODUCED USING TWO METHODS

Marcin NABIAŁEK, Kinga JEŻ\*

Institute of Physics, Faculty of Production Engineering and Materials Technology,  
Czestochowa University of Technology, 19 Armii Krajowej Str., 42-200 Czestochowa, Poland.

### Abstract

*The article presents results of investigations of the structure and selected magnetic properties of a bulk amorphous alloy with the chemical composition Fe<sub>39</sub>Co<sub>33</sub>Y<sub>8</sub>B<sub>20</sub>. Alloy was produced using two methods: injection suction liquid alloy into a water-cooled copper mold. Structure of the materials was examined using X-ray diffraction. Magnetic properties were determined on the basis of measurements by the vibration magnetometer and the Faraday magnetic weight. Alloy samples produced were characterized by high Curie temperature (over 700 K) and soft magnetic properties, i.e. high saturation magnetization (1.1 T) and low coercive field value (below 200 A/m). On the basis of the primary magnetisation curves, the type of defects occurring in the samples of manufactured alloys was determined and the spin wave stiffness parameter was determined.*

**Keywords:** bulk metallic glasses, soft magnetic, injection method, suction-casting method, approach to ferromagnetic saturation.

### Introduction

Amorphous materials are an interesting object of research due to their unusual properties. Often, the properties of amorphous materials are better than their crystalline equivalent, with the same chemical composition [1]. A relatively new group of materials are the so-called bulk amorphous materials [2, 3]. A particularly interesting group are amorphous iron-based alloys. These materials are characterized by so-called soft magnetic properties, including high magnetisation of saturation value, high magnetic permeability or low coercive field [4, 5]. In amorphous materials there are defects of the structure under a slightly different form than in crystalline materials. In the case of amorphous materials, these defects take the form of free volumes and pseudodyslocation dipoles. There are no direct methods for observing them. Their presence in the material can be determined based on the analysis of the primary magnetization curves in accordance with the theory of H. Kronmüller [6-11]. According to its assumptions, magnetizations can be described by dependence:

$$\mu_0 M(H) = \mu_0 M_s \left[ 1 - \frac{a_{1/2}}{(\mu_0 H)^{1/2}} - \frac{a_1}{(\mu_0 H)^1} - \frac{a_2}{(\mu_0 H)^2} \right] + b(\mu_0 H)^{1/2} \quad (1)$$

Where:  $M_s$  - spontaneous magnetization,  $\mu_0$  - vacuum magnetic permeability,  $H$  - magnetic field,  $a_i$  ( $i = 1/2, 1, 2$ ) - angular linear adjustment coefficients, which correspond to free volume and linear defects,  $b$  - slope of a linear fit corresponding to thermal attenuation excited spin waves damping in a high intensity magnetic field.

The factors in equation (1) can be described as follows:

$$\frac{a_{1/2}}{(\mu_0 H)^{1/2}} = \mu_0 \frac{3}{20A_{ex}} \left( \frac{1+r}{1-r} \right)^2 G^2 \lambda_s^2 (\Delta V)^2 N \left( \frac{2A_{ex}}{\mu_0 M_s} \right)^{1/2} \frac{1}{(\mu_0 H)^{1/2}} \quad (2)$$

$$\frac{a_1}{\mu_0 H} = 1,1 \mu_0 \frac{G^2 \lambda_s^2}{(1-\nu)^2} \frac{Nb_{eff}}{M_s A_{ex}} D_{dip}^2 \frac{1}{\mu_0 H} \quad (3)$$

$$\frac{a_2}{\mu_0 H^2} = 0,456 \mu_0 \frac{G^2 \lambda_s^2}{(1-\nu)^2} \frac{Nb_{eff}}{M_s^2} D_{dip}^2 \frac{1}{(\mu_0 H)^2} \quad (4)$$

Where:  $\Delta V$  – volume change caused by the occurrence of a point defect characterized by density  $N$ ,  $A_{ex}$  - exchange constant,  $G$  - cross flexible shear module,  $r$  – Poissona coefficients,  $\lambda_s$  - magnetostriction constant.

Equation (2) describes the influence of free volumes on the magnetisation process while the remaining equations concern the impact of linear defects on the process, where equation (3) describes these defects for the assumption of  $D_{dip} < l_H$ , and the dependence (4) for  $D_{dip} > l_H$  where  $l_H$  is the distance the least two dipoles. The magnetizing process above this area is related to the thermally excited spin waves damping, the process can be characterized by the parameter  $b$ :

$$b = 3,54 g \mu_0 \mu_B \left( \frac{1}{4\pi D_{spf}} \right)^{3/2} kT (g \mu_B)^{1/2} \quad (5)$$

Where:  $k$  – Boltzman constant,  $\mu_B$  – Bohr magneton,  $g$  – gyromagnetic coefficient.

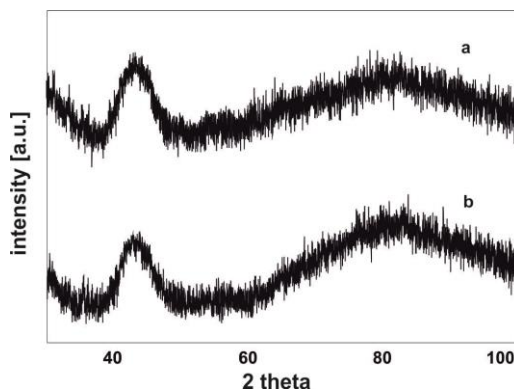
The aim of the work was to examine the structure and properties of a massive amorphous alloy with chemical composition  $Fe_{39}Co_{33}Y_8B_{20}$  produced using two production methods: injection and suction of a liquid alloy into a water-cooled copper mold.

## Material and Methods

The polycrystalline ingot was made using an arc furnace under a protective atmosphere of argon with components having a purity of 99.9 %. Bulk amorphous alloy was produced using two methods: injection and suction liquid alloy into the copper mold. These methods have a similar cooling rate of up to  $10^3$  K s. Samples of the materials were produced at the same pressure of protective gas prevailing in the working chamber, identical copper forms were used. The alloy was cast in the form of  $10 \times 5 \times 0.5$  mm plates. The methods differ in terms of melting the charge and the introduction of a liquid alloy into the copper mold. In addition, in the case of the suction method, prior to the alloy casting process, pure titanium was melted to capture the remaining impurities in the working chamber. The structure of the prepared samples was examined using a BRUCKER X-ray diffractometer equipped with a  $CuK\alpha$  lamp. The study was carried out in the range of  $30 - 100^\circ$  two theta. Thermomagnetic curves were measured using a Faraday magnetic balance. The primary magnetization curves and static magnetic hysteresis loops were measured using a LakeShore vibration magnetometer in the magnetic field range up to 2T. Primary magnetization curves were analyzed in accordance with the assumptions of H. Kronmüller theory.

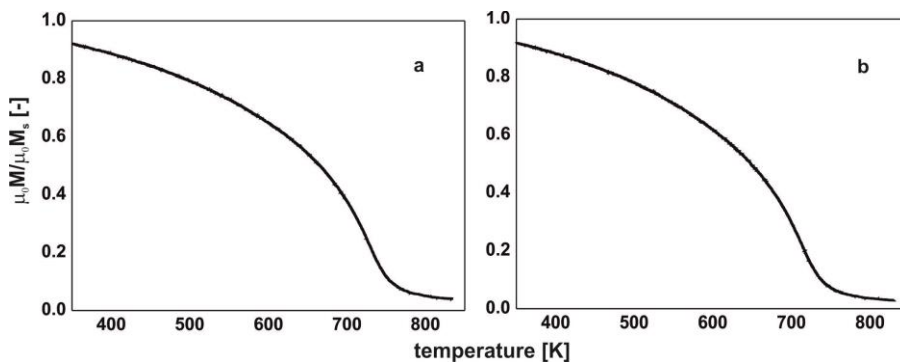
## Results

Fig. 1 presents X-ray diffractograms measured for  $\text{Fe}_{39}\text{Co}_{33}\text{Y}_8\text{B}_{20}$  alloy produced using two methods.



**Fig. 1.** X-ray diffractograms measured for  $\text{Fe}_{39}\text{Co}_{33}\text{Y}_8\text{B}_{20}$  alloy produced using the method: a) suction, b) injection

Recorded x-ray diffraction images are typical of amorphous materials. For the two samples tested, wide maximum in the range of  $40 - 50^\circ$  two theta showing the reflection of X-rays from the chaotically distributed atoms in the volume of the sample are visible. Fig. 2 shows the reduced magnetic saturation polarization curves as a function of temperature.



**Fig. 2.** Magnetic saturation polarization curves as a function of temperature measured for  $\text{Fe}_{39}\text{Co}_{33}\text{Y}_8\text{B}_{20}$  alloy produced using the method: a) suction, b) injection

The measurement was carried out in the range from room temperature to 850K. In the test range, one of the gentle inflection associated with the transition of the magnetic phase from the ferro to the paramagnetic state is visible for both tested alloy samples. This phase is an amorphous matrix identified on the basis of diffractograms (Fig. 1). The magnetization drops almost to 0, which confirms the absence of other magnetic phases in the studied range. For ferromagnetics that meet the Heisenberg assumptions, it is possible to determine the Curie temperature using the critical coefficient  $\beta = 0.36$ . The numerical analysis of magnetic saturation polarization curves as a function of temperature is shown in Fig. 3.

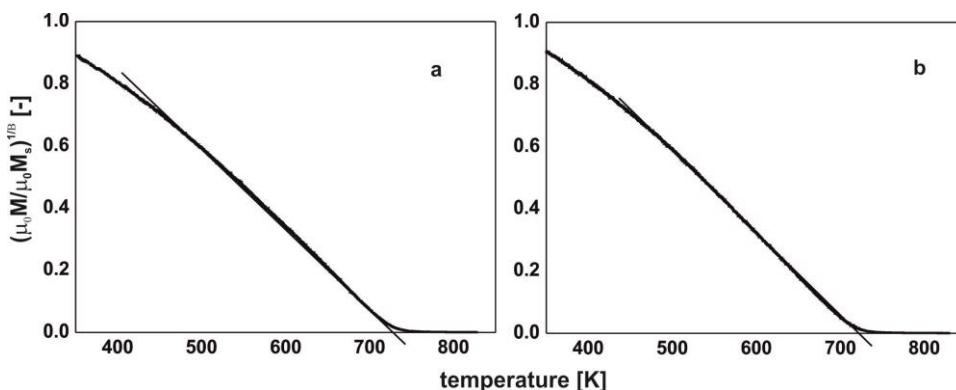


**Fig. 3.** Determined Curie temperature for Fe<sub>39</sub>Co<sub>33</sub>Y<sub>8</sub>B<sub>20</sub> alloy produced using the method: a) suction, b) injection

The Fe<sub>39</sub>Co<sub>33</sub>Y<sub>8</sub>B<sub>20</sub> alloy produced by the suction method is characterized by a Curie temperature of 725K, while the alloy is produced by the 720K injection method. Fig. 4 shows the static magnetic hysteresis loops measured at the intensity of the external magnetic field up to 2T.

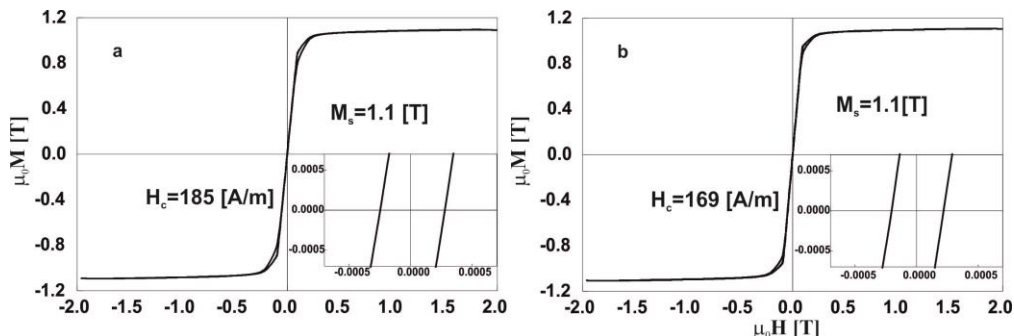


**Fig. 4.** Static magnetic hysteresis loops measured for Fe<sub>39</sub>Co<sub>33</sub>Y<sub>8</sub>B<sub>20</sub> alloy produced using the method: a) suction, b) injection

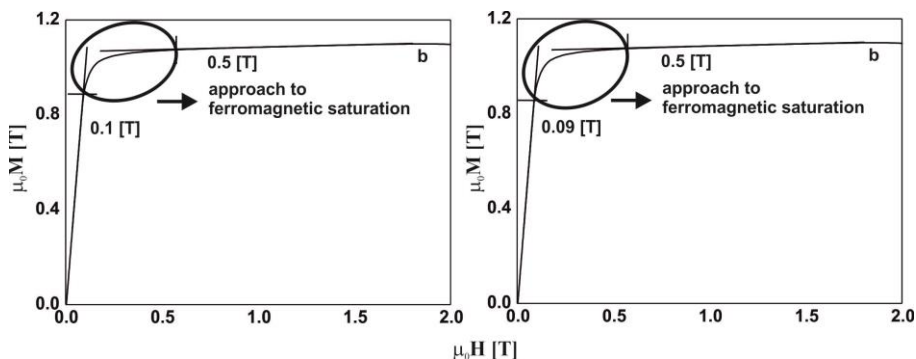


**Fig. 5.** The primary magnetization curves measured for the alloy Fe<sub>39</sub>Co<sub>33</sub>Y<sub>8</sub>B<sub>20</sub> produced using the method: a) suction, b) injection

Static magnetic hysteresis loops registered for the Fe<sub>39</sub>Co<sub>33</sub>Y<sub>8</sub>B<sub>20</sub> alloy are typical for materials with soft magnetic properties. The alloy samples produced using different methods have the same saturation magnetization value (1.1T) and a similar value of the coercive field

(169 and 185 A/m). Thus, no significant influence of the production method on the magnetic properties of the  $\text{Fe}_{39}\text{Co}_{33}\text{Y}_8\text{B}_{20}$  alloy was noticed. Fig. 5 presents the primary magnetization curves measured for samples of the alloy produced. The course of the primary magnetisation curves for both alloy samples is very similar. The area so-called the approach to ferromagnetic saturation was pre-determined. The primary magnetisation curves were analyzed. Fig. 6 shows the relationship  $\mu_0 M(\mu_0 H^{-2})$ .

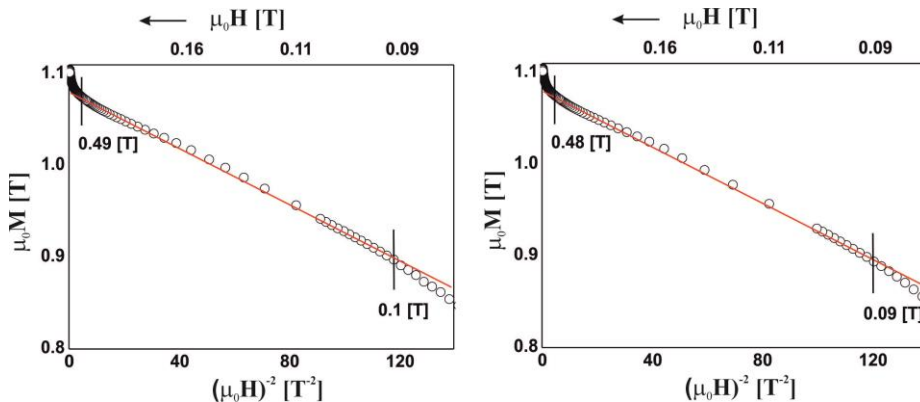


Fig. 6. Dependence  $\mu_0 M(\mu_0 H^{-2})$  for the alloy  $\text{Fe}_{39}\text{Co}_{33}\text{Y}_8\text{B}_{20}$  produced using the method: a) suction, b) injection

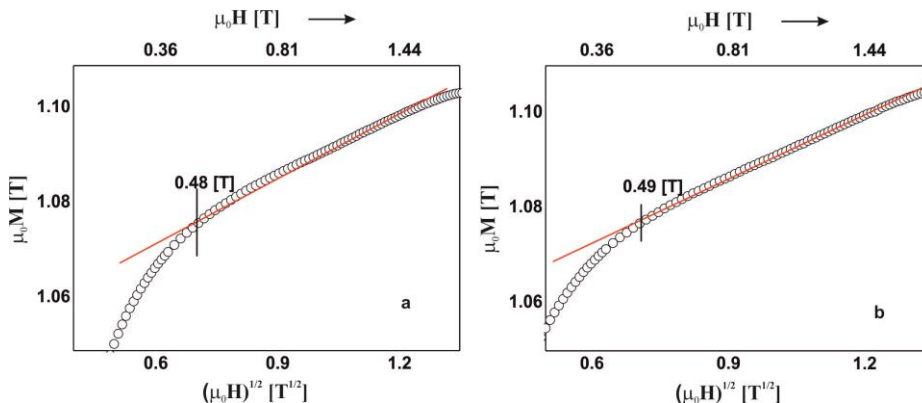


Fig. 7. Dependence  $\mu_0 M(\mu_0 H^{1/2})$  for the alloy  $\text{Fe}_{39}\text{Co}_{33}\text{Y}_8\text{B}_{20}$  produced using the method: a) suction, b) injection

After analyzing the curves according to the H. Kronmüller theory, it turned out that the course of the magnetisation process of both samples is similar. In the magnetic field from about 0.1T to about 0.5T, the magnetisation process is related to the rotation of the magnetisation vector around the linear defects of the structure. Fig. 7 presents the primary magnetization curves in the intensity of the magnetic field above the area of approach to ferromagnetic saturation in function  $(\mu_0 H^{1/2})$ . In this area, the magnetising process is associated with the damping of thermally excited spin waves. On the basis of curve analysis in this range, the spin wave stiffness parameter  $D_{\text{spf}}$  can be determined. For the alloy produced by the suction method, this parameter is 49.7 meVnm<sup>2</sup> and for the sample produced by the injection method: 50.3 meVnm<sup>2</sup>.

## Conclusions

The methods of injection and suction the liquid alloy into the copper mold allow for the production of bulk amorphous alloys on the iron matrix. The alloy samples produced were characterized by a high Curie temperature (over 700 K). It is worth paying attention on the slightly higher Curie temperature value for the alloy produced by the suction method. Higher Curie temperature can be associated with the formation of another degree of disordering the structure during solidification of the alloy. Fe<sub>39</sub>Co<sub>33</sub>Y<sub>8</sub>B<sub>20</sub> alloy samples were characterized by so-called soft magnetic properties. The method of placing a liquid alloy in copper form has no significant effect on the magnetization of saturation value and the coercive field value. The tested alloy undergoes the process of magnetising in an almost identical way, regardless of the production method as indicated by the analysis of the primary magnetisation curves and the D<sub>spf</sub> parameter. On the basis of the curve analysis, point defects were not identified. However, this does not exclude their presence in the volume of samples produced. The influence of free volumes on the magnetizing process is much smaller than in the case of linear defects. In the case of a large number of pseudo-location dipoles, the effect of free volumes may be impossible to observe. In this case, the presence of free volumes can be confirmed by measuring the magnetic susceptibility dissaccomodation.

## References

- [1] A. Inoue, N. Yano and T. Masumoto, *Production of metal-zirconium type amorphous wires and their mechanical strength and structural relaxation*, **J. Mater. Science**, **19**, 1984, pp. 3786-3795.
- [2] A. Inoue, T. Zhang and T. Masumoto, *Zr-Al-Ni Amorphous Alloys with High Glass Transition Temperature and Significant Supercooled Liquid Region*, **Materials Transactions JIM**, **31**, 1990, pp. 177-183.
- [3] A. Inoue, A. Kato, T. Zhang, S.G. Kim and T. Masumoto, *Mg-Cu-Y Amorphous Alloys with High Mechanical Strengths Produced by a Metallic Mold Casting Method*, **Materials Transaction JIM**, **32**, 1991, pp. 609-616.
- [4] G. Herzer, *Modern soft magnets: Amorphous and nanocrystalline materials*, **Acta Materialia**, **61**, 2013, pp. 718–734.
- [5] A. Inoue, *Bulk amorphous alloys with soft and hard magnetic properties*, **Materials Science and Engineering A**, **226-228**, 1997, pp. 357-363.
- [6] H. Kronmüller, M. Fahnle, H. Grimm, R. Grimm and B. Groger, *Magnetic properties of amorphous ferromagnetic alloys*, **J. Magn. Magn. Mater.**, **13**, 1979, pp. 53-70.
- [7] H. Kronmüller, *General Micromagnetic Theory, Handbook of Magnetism and Advanced Magnetic Materials*, **John Wiley&Sons**, **2**, 2007, pp. 703-739.
- [8] K. Bloch, *Microstructure and High-Field Magnetic Properties of Fe-Based Bulk Amorphous Alloys*, **Revista de Chimie**, **69(4)**, 2018, pp. 982-985.
- [9] K. Bloch, M.A. Titu, A.V. Sandu, *Investigation of the Structure and Magnetic Properties of Bulk Amorphous FeCoYB Alloys*, **Revista de Chimie**, **68(9)**, 2017, pp. 2162-2165.
- [10] K. Bloch, *The Influence of Isothermal Annealing and Structural Defects on Properties of Amorphous Fe<sub>78</sub>Si<sub>11</sub>B<sub>11</sub> with High Magnetization Saturation*, **Revista de Chimie**, **68(3)**, 2017, pp. 478-482.
- [11] K. Gruszka, M. Nabialek, M. Szota, P. Vizureanu, M.M.A. Abdullah, K. Bloch, A.V. Sandu, *The Study of Magnetization in Strong Magnetic Fields for Fe<sub>62-x</sub>CO<sub>10</sub>Nb<sub>x</sub>Y<sub>8</sub>B<sub>20</sub> (X=0, 1, 2) Alloys*, **Revista de Chimie**, **68(2)**, 2017, pp. 265-268.

Received: December 6, 2018

Accepted: January 10, 2019